

Optical near-zone-center phonons and their interaction with electrons in $\text{YBa}_2\text{Cu}_3\text{O}_7$: Results of the local-density approximation

C. O. Rodriguez, A. I. Liechtenstein,* I. I. Mazin,[†] O. Jepsen, and O. K. Andersen
Max-Planck-Institut für Festkörperforschung, D-7000 Stuttgart 80, Federal Republic of Germany

M. Methfessel

Fritz-Haber-Institut, Faradayweg 4-6, D-1000 Berlin 33, Federal Republic of Germany

(Received 2 May 1990)

Ab initio frozen-phonon calculations were performed for $\text{YBa}_2\text{Cu}_3\text{O}_7$ for the five A_g Raman-active and for two B_{1u} infrared-active optical $\mathbf{q}=\mathbf{0}$ modes, with use of the local-density approximation and the full-potential linear-muffin-tin-orbital method. The full A_g dynamical matrix was calculated using 98 \mathbf{k} points in the $\frac{1}{8}$ Brillouin zone. The theoretical and experimental equilibrium structures and phonon frequencies ω_v agree well. Phonon linewidths $\gamma_{v\mathbf{q}}$, due to electronic intraband transitions in the normal state, and electron-phonon coupling constants $\lambda_{v\mathbf{q}} \equiv \gamma_{v\mathbf{q}}/[\pi N(0)\omega_v^2]$ were calculated for the A_g modes and small, transverse \mathbf{q} . We estimate that $\lambda \approx 1$ for the sum over all modes. The phonon shifts and broadenings observed for $T < T_c$ by Raman scattering are well accounted for by conventional strong-coupling theory and our calculated electron-phonon coupling.

For the high-temperature superconductors not only the mechanism of superconductivity is unknown but also the proper description of their electronic structure in the normal state is under dispute. Contrary to earlier belief, it now seems that for the metallic compounds a Fermi-liquid picture is appropriate and even that the bands calculated using the local-density-functional approximation (LDA) may be relevant. Recent angle-resolved photoemission experiments,¹ for instance, have given points on the Fermi surface in $\text{YBa}_2\text{Cu}_3\text{O}_7$ which agree reasonably with those of earlier LDA calculations.² The LDA, furthermore, reproduces the x-ray-absorption spectra of $\text{YBa}_2\text{Cu}_3\text{O}_7$ rather well.³

It is generally accepted that the LDA accounts for the total energy of a solid and, hence, for the structural and lattice-dynamical properties (in the adiabatic approximation). This was recently⁴ shown to also hold for La_2CuO_4 . Now, it is of interest to consider $\text{YBa}_2\text{Cu}_3\text{O}_7$, the best characterized high-temperature superconductor, because such an LDA frozen-phonon calculation, if successful, could also provide insight to the magnitude of the electron-phonon (EP) coupling, the agent for conventional superconductivity. That the EP coupling may be strong and even play some role for the high-temperature superconductivity was recently speculated on the basis of Raman-scattering experiments^{5,6} showing that, for certain phonons, the frequencies and linewidths change as the temperature is lowered below T_c , and that the corresponding resonances in the Raman spectra have Fano shapes.

In this paper we present results for $\text{YBa}_2\text{Cu}_3\text{O}_7$ of such an *ab initio* frozen-phonon calculation in the LDA. We consider optical, near-zone-center phonons and calculate, for the five A_g Raman-active modes, the frequencies and eigenvectors, the influence of metallic screening, the wave-vector dependent phonon linewidths $\gamma_{v\mathbf{q}}$ for small \mathbf{q} , the corresponding partial EP coupling constants $\lambda_{v\mathbf{q}}$ and the changes of the phonon frequencies and linewidths in

the superconducting state, as given by conventional strong-coupling theory.⁷ Finally, we present frequencies for two infrared-active B_{1u} modes.

We used a newly developed fast and precise full-potential linear muffin-tin-orbital (FP-LMTO) technique which makes no shape approximation for the charge density or for the potential.⁸ The basis set included 204 LMTO's per cell and yielded an accuracy of energy bands and total energies beyond 10 meV. Moreover, in the self-consistent calculations it was necessary to use 98 or 147 \mathbf{k} points plus linear tetrahedral interpolation in the irreducible Brillouin zone (BZ) of the orthorhombic structure. This high accuracy and many \mathbf{k} points are necessary to properly describe the EP interaction.

The total energy was first calculated as a function of the volume and the c/a ratio. In Table I we compare the measured⁹ and calculated static structural parameters. The calculated cell volume is 5% smaller than the volume measured at 103 K.¹⁰ An overbinding of this magnitude was also found for La_2CuO_4 (Ref. 4) and is common for transition metals and their compounds and is ascribed to the LDA. For the frozen-phonon calculation, to be described in the following, we used the experimental equilibrium volume and c/a ratio.

The five Raman-active A_g modes displace apical oxygen O(4), Ba, plane copper Cu(2), and plane oxygens O(2) and O(3) in the c direction. In order to determine the equilibrium positions of these five atoms and the dynamical

TABLE I. Static structural parameters.

	$V(\text{\AA}^3)$	c/a	O(4)	Ba	z/c_{exp}		
					Cu(2)	O(2)	O(3)
EXP ^a	173.5	3.05	0.158	0.184	0.356	0.377	0.379
LDA	163.1	3.02	0.157	0.184	0.355	0.375	0.375

^a $T = 300$ K, Ref. 9.

cal matrix, we calculated the total energies for 28 different displacement patterns (even with respect to the Y site) including those of individual atoms as well as mixed displacements. The atomic displacements were about 0.07 Å. The total energies were least-squares fitted, first to a polynomial quadratic in the five displacements, and thus containing 21 terms. We checked the stability of this fit by excluding some of the 28 patterns and by adding several cubic terms. The coefficients of the linear and quadratic terms did not change appreciably, except for the submatrix concerning the displacements of O(2) and O(3). Our final fit was quadratic with two additional cubic terms: $O(2)^2[O(3)+O(2)]$ and $O(3)^2[O(3)+O(2)]$. The equilibrium positions thus obtained for the five atoms are in excellent agreement with experiment (Table I). Even the so-called dimpling of the CuO_2 planes is accurately reproduced. The phonon frequencies ω_ν and eigenvectors $e_{i\nu}$ obtained from the eigenvalues and eigenvectors of the dynamical matrix are displayed in Table II. The agreement between the experimental and theoretical frequencies is satisfactory, the latter being 10% softer, except for the 330 cm^{-1} mode. Calculations for a reduced cell volume yielded Grüneisen parameters $d\ln\omega/d\ln V$ of about two, which compare well with the experimental values 1.5–1.9,¹¹ and a rescaling of the dynamical matrix to the theoretical equilibrium volume gives calculated frequencies in even better agreement with experiment.

A previous assignment of the A_g modes from lattice dynamical calculations using empirical interatomic force constants¹² was, in order of increasing phonon frequencies: Ba, Cu(2), $0.8[O(3)-O(2)]+0.2[O(3)+O(2)]$, $0.2[O(3)-O(2)]+0.8[O(3)+O(2)]$, O(4). Here, O(3)–O(2) and O(3)+O(2) indicate, respectively, out-of-phase and in-phase movements of the plane oxygens. Our *ab initio* calculations confirm this with a few modifications: (i) the two highest modes (500 and 440 cm^{-1}) show about 20% mixing of, respectively, $[O(3)+O(2)]$ and O(4) motion, (ii) the two lowest modes involve approximately equal mixtures of Ba and Cu(2) vibrations. The reason for the latter mixing is that the “pure” modes are nearly degenerate in our calculations, but the coupling between Cu(2) and Ba in the dynamical matrix is not particularly strong. Indirect experimental information on the phonon eigenvectors can be inferred from the polarization dependences of the Raman intensities. This analysis was used to conjecture that the 330 cm^{-1} mode has approximately O(3)–O(2) symmetry⁶ and that the 440 cm^{-1} mode includes some O(4) admixture,¹³ as indeed we find. Interestingly, the polarization dependence of the two

lowest modes are similar⁶ and this may support our conjecture that they are not purely Ba and Cu(2) modes. On the other hand, isotope substitution of Cu does not influence the 110 mode¹⁴ and this contradicts our eigenvectors. We speculate that although our calculations may overestimate the coupling, at least 20% admixture will exist.

In addition to the A_g modes we have calculated the frequencies for two B_{1u} modes, the “Ba”-mode 140 cm^{-1} ($\omega_{\text{exp}}=150$) and “Y”-mode 200 cm^{-1} ($\omega_{\text{exp}}=190$) taking over the eigenvectors from the empirical calculations.¹⁵

The second part of our work deals with the coupling of the A_g phonons to the electrons. The basic quantity defining this interaction is the EP matrix element

$$g_{\nu,n\mathbf{k},m(\mathbf{k}+\mathbf{q})} \equiv \langle n\mathbf{k} | V'_{i\nu\mathbf{q}} | m(\mathbf{k}+\mathbf{q}) \rangle / \sqrt{2\omega_{\nu\mathbf{q}}},$$

where ν and \mathbf{q} are the phonon branch and wave vector, respectively. $|n\mathbf{k}\rangle$ is a quasiparticle state for the undistorted crystal and

$$V'_{i\nu\mathbf{q}}(\mathbf{r}) = \sum_i (e_{i\nu\mathbf{q}}/\sqrt{M_i}) \delta V(\mathbf{r})/\delta R_i$$

is the variation of the self-consistent potential caused by the phonon distortion. Index i runs over the atoms and, for each atom, over the three cartesian coordinates. Knowing g one can, in principle, calculate both the influence of the electrons on phonons (e.g., phonon linewidths), and the influence of phonons on electrons (e.g., the Eliashberg spectral function which enters the conventional theory of superconductivity). The full information is contained in the EP coupling constant¹⁶

$$\lambda_{\nu\mathbf{q}} = \frac{2}{\omega_{\nu\mathbf{q}}N(0)} \times \sum_{n,m,\mathbf{k}} |g_{\nu,n\mathbf{k},m(\mathbf{k}+\mathbf{q})}|^2 \delta(\epsilon_{n\mathbf{k}}) \delta(\epsilon_{m(\mathbf{k}+\mathbf{q})} - \epsilon_{n\mathbf{k}} - \omega_{\nu\mathbf{q}}),$$

where $\epsilon_{n\mathbf{k}}$ are the quasiparticle energies relative to the Fermi level and $N(0) = \sum_{n\mathbf{k}} \delta(\epsilon_{n\mathbf{k}}) = 2.0$ states/(YBa₂Cu₃O₇ spin eV) is the density of states per spin at ϵ_F ($\equiv 0$). The two δ functions reduce the \mathbf{k} sum to a line integral at the Fermi surface. Summing $\lambda_{\nu\mathbf{q}}$ over the 39 phonon branches ν and averaging it over \mathbf{q} in the Brillouin zone gives the standard EP coupling constant λ . Finally, the phonon linewidth, which can be measured by neutron scattering, is given by $\gamma_{\nu\mathbf{q}} = \pi N(0) \omega_{\nu\mathbf{q}}^2 \lambda_{\nu\mathbf{q}}$. For optical phonons and $q=0$, interband transitions may be neglected since they are allowed only at isolated points on the Fermi

TABLE II. Frequencies, eigenvectors, and EP coupling constants for the A_g $q=0$ phonons.

$\omega_\nu(\text{cm}^{-1})$	$e_{i\nu}$						$\lambda_\nu(\%)$	
	EXP ^a	LDA	Ba	Cu(2)	O(3)–O(2)	O(3)+O(2)		O(4)
110	95		0.65	0.75	0.05	0.07	–0.07	3.4
150	130		0.76	–0.65	–0.02	–0.02	0.04	0.7
330	330		–0.01	–0.02	0.89	–0.43	–0.14	2.1
440	400		–0.02	–0.04	0.44	0.76	0.47	1.0
500	460		0.03	0.11	–0.10	–0.48	0.87	0.9

^aReference 6.

surface. As q increases, the first interband transitions are those between the two Fermi surface sheets from the plane bands but, for the A_g phonons, these transitions are essentially forbidden. For small q , the relative phonon linewidth may then be reduced to the intraband contribution

$$\gamma_{vq}/\omega_v = 2\pi \sum_{n,\mathbf{k}} |g_{v,n\mathbf{k},n\mathbf{k}}|^2 \delta(\varepsilon_{n\mathbf{k}}) \delta(\mathbf{q} \cdot \mathbf{v}_{n\mathbf{k}} - \omega_v),$$

where $\mathbf{v}_{n\mathbf{k}}$ are the Fermi velocities and we have assumed the existence of a $q=0$ limit for the EP matrix elements. This assumption holds when the screening is metallic in all directions, or if we consider transverse phonons (i.e., if, in the present case, $q_c=0$). The EP matrix elements may then be obtained from the deformation potentials relative to the Fermi energy

$$g_{v,n\mathbf{k},n\mathbf{k}} = \sum_i (e_{iv}/\sqrt{2M_i\omega_v}) \partial \varepsilon_{n\mathbf{k}} / \partial R_i.$$

Figure 1 shows γ_{vq}/ω_v and λ_{vq} as functions of q_{ab} for $q_c=0$ and averaged over the angles in the ab plane. Had the Fermi surface been a cylinder with velocity v_{ab} , the

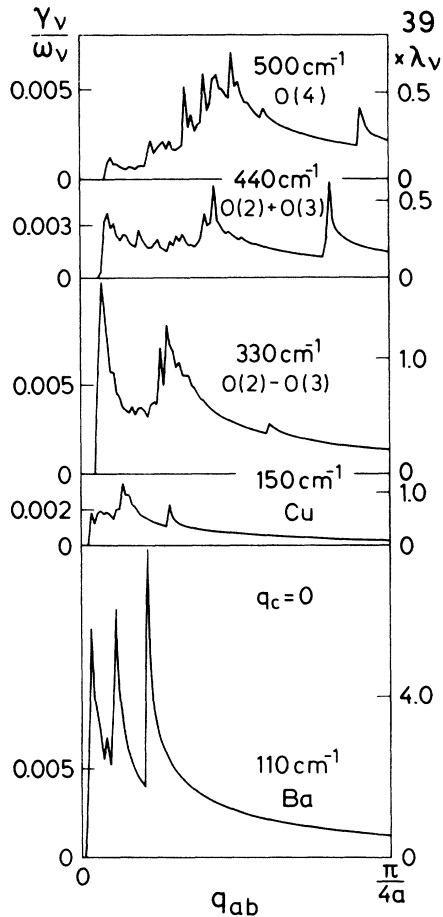


FIG. 1. Calculated intraband contribution to the relative phonon linewidths, γ_{vq}/ω_v , and partial coupling constants, λ_{vq} , for the five A_g optical phonons. The wave-vector \mathbf{q} is in the ab plane and the average has been taken over the angles in the plane so that $q_{ab} \equiv |\mathbf{q}|$. The λ 's have been multiplied by the total number of phonon branches.

q_{ab} dependence of γ_v or λ_v would have been proportional to $x^{1/2}\theta(x)$ with $x \equiv (v_{ab}q_{ab})^2 - \omega_v^2$. The 110-cm $^{-1}$ mode is seen to have the largest λ_v . This is due to the $\approx 50\%$ mixing with the Cu(2) mode. Since the Cu mass is about half the Ba mass, Cu oscillates with a larger amplitude in both of the lowest modes, and their λ_v 's are mainly due to the Cu(2) deformation potential and only to a minor extent to Ba. The 110 mode has the larger λ_v because its frequency is lower. This result is consistent with the fact that the 110 mode was found⁵ to have a highly asymmetric Raman line shape (Fano resonance). The next strongest Fano resonance was found for the 330 mode.⁵ We find that this phonon, as well as the 440 phonon, due to the presence of the dimple, modulate the Cu(2)-O(2) and Cu(2)-O(3) $pd\sigma$ hopping integrals and thus move the plane-band saddle points near X and Y , which are merely 20 meV below ε_F and which give the main contribution to the density of states. The 440 mode has the smaller λ_v because its frequency is higher and because its deformation potentials are smaller. The reason for the latter is that the Fermi level can follow an in-phase movement of the bands near X and Y but not an out-of-phase movement. The 500 mode has a good-sized λ_v despite its high frequency, since the O(4) movement is in the direction of the O(4)-Cu(1) $pd\sigma$ orbital and therefore strongly modifies the position of the chain band and, hence, the position of the Fermi level with respect to the saddle points of the plane bands. By taking the small- q average of the λ_{vq} curves, by averaging over the five A_g modes, and by multiplying by the total number of modes (39), one may estimate a total λ of order 1.

A quantity of interest related to the EP interaction is the softening of the phonon frequencies due to metallic screening. The one-electron contribution to the dynamical matrix is proportional to

$$\sum_{n,\mathbf{k}} [\varepsilon_{n\mathbf{k}} \theta(-\varepsilon_{n\mathbf{k}})]_{ij}'' = \sum_{n,\mathbf{k}} \varepsilon_{ijn\mathbf{k}}'' \theta(-\varepsilon_{n\mathbf{k}}) - \sum_{n,\mathbf{k}} \varepsilon'_{in\mathbf{k}} \varepsilon'_{jn\mathbf{k}} \delta(\varepsilon_{n\mathbf{k}}),$$

where $\varepsilon'_i \equiv \partial/\partial R_i$. The second term is the Fermi-surface contribution which gives rise to a relative change of phonon frequencies

$$\Delta \omega_v^{FS}/\omega_v = -(2/\omega_v) \sum_{n,\mathbf{k}} |g_{v,n\mathbf{k},n\mathbf{k}}|^2 \delta(\varepsilon_{n\mathbf{k}}) \equiv -\lambda_v^s.$$

Our calculated softenings, listed in Table II, are of the order of the difference between phonon frequencies calculated using 98 \mathbf{k} points and only 9 \mathbf{k} points.

The λ_v^s just calculated also gives the magnitude of the change of the phonon self-energy due to transitions across the gap in the superconducting state. The relative change may be expressed as

$$\Delta \Sigma_v/\omega_v \equiv (\Delta \omega_v/\omega_v) - i(\Delta \gamma_v/\omega_v) = \lambda_v^s F[\omega_v/2\Delta(T)],$$

where $2\Delta(T)$ is the superconducting gap. In the simple BCS theory, $F(\tilde{\omega}) = -u/\sin u$, with $u \equiv \pi - 2\cos^{-1}(\tilde{\omega})$ or $\pi + 2i \cosh^{-1}(\tilde{\omega})$, according to whether $\tilde{\omega} \equiv \omega_v/[2\Delta(T)]$ is smaller or greater than unity. In the strong-coupling regime, $F(\tilde{\omega})$ has a similar behavior.⁷ Recent Raman experiments found such an effect: softening of the 330-cm $^{-1}$ mode and hardening of the 440-cm $^{-1}$ mode.¹⁷ The

experimental estimate of λ_{ν}^{ν} (taking $2\Delta/kT_c \approx 5.2$),¹⁷ agrees well with our *ab initio* values of 2% for the 330 mode and 1% for the 440 mode. Increased phonon linewidths also follow from this theory,⁷ but are more difficult to observe experimentally. Available data⁵ for the 330 mode are in accord with our $\lambda_{\nu}^{\nu}=2\%$ and $2\Delta/kT_c=5.2$.

In summary, we have performed LDA frozen-phonon calculations of the full dynamical matrix for the A_g $q=0$ phonons in $\text{YBa}_2\text{Cu}_3\text{O}_7$. The calculated frequencies agree well with Raman experiments. Also the calculated eigenvectors are consistent with most experimental observations. We have investigated the influence of the metallic screening by calculating directly the Fermi-surface contribution to the dynamical matrix. The coupling of the elec-

trons to the A_g phonons was calculated self-consistently in the adiabatic approximation and phonon linewidths $\gamma_{\nu q}$ and partial coupling constants $\lambda_{\nu q}$ were evaluated for small q . The coupling was found to be particularly large for the 110 and 330- cm^{-1} modes. The total λ summed over all modes was estimated to be approximately one. Assuming a strong-coupling pairing, we calculated the magnitude of the softenings and hardenings of the A_g Raman modes below T_c , and found good agreement with experiment.

We have benefited from discussions with M. Cardona, W. Kress, D. Rainer, C. Thomsen, J. Zaanen, and R. Zeyher. C.O.R. and I.I.M. acknowledge partial financial support from the A. von Humboldt Foundation.

*Permanent address: Institute of Chemistry, Sverdlovsk, U.S.S.R.

†Permanent address: P. N. Lebedev Physical Institute, Moscow, U.S.S.R.

¹J. C. Campuzano, G. Jennings, M. Faiz, L. Beaulaigue, B. W. Veal, J. Z. Liu, A. P. Paulikas, K. Vandervoort, H. Claus, R. S. List, A. J. Arko, and R. J. Bartlett, *Phys. Rev. Lett.* **64**, 2308 (1990).

²J. Yu, S. Massida, A. J. Freeman, and D. D. Koelling, *Phys. Lett. A* **122**, 203 (1987).

³J. Zaanen, M. Alouani, and O. Jepsen, *Phys. Rev. B* **40**, 837 (1989).

⁴R. E. Cohen, W. E. Pickett, and H. Krakauer, *Phys. Rev. Lett.* **62**, 831 (1989).

⁵S. L. Cooper, M. V. Klein, B. G. Pazol, J. P. Rice, and D. M. Ginsberg, *Phys. Rev. B* **37**, 5920 (1988).

⁶C. Thomsen and M. Cardona, in *Physical Properties of High-Temperature Superconductors*, edited by D. M. Ginsberg (World Scientific, Singapore, 1989).

⁷R. Zeyher and G. Zwirnagl, *Z. Phys. B* **78**, 175 (1990).

⁸M. Methfessel, C. O. Rodriguez, and O. K. Andersen, *Phys. Rev. B* **40**, 2009 (1989).

⁹M. A. Beno, L. Soderholm, D. W. Capone II, D. E. Hinks, J. D. Jorgensen, J. D. Grace, I. K. Schuller, C. U. Segre, and K. Zhang, *Appl. Phys. Lett.* **51**, 57 (1987).

¹⁰A. Simon, J. Köhler, H. Borrmann, B. Gegenheimer, and R. Kremer, *J. Solid. State Chem.* **77**, 200 (1988).

¹¹K. Syassen, M. Hanfland, K. Strössner, M. Holtz, and W. Kress, M. Cardona, U. Schröder, J. Prade, A. D. Kulkarni, and F. W. de Wette, *Physica C* **153**, 264 (1988).

¹²W. Kress, U. Schröder, J. Prade, A. D. Kulkarni, and F. W. de Wette, *Phys. Rev. B* **38**, 2906 (1988).

¹³E. I. Rashba and E. Y. Sherman (unpublished).

¹⁴A. Mascarenhas, H. Katayama-Yoshida, J. Pankove, and S. K. Deb, *Phys. Rev. B* **39**, 4699 (1989).

¹⁵L. Genzel, A. Wittlin, H. Bauer, M. Cardona, E. Schönherr, and A. Simon, *Phys. Rev. B* **40**, 2170 (1989).

¹⁶D. Rainer, *Prog. Low Temp. Phys.* **10**, 371 (1986).

¹⁷C. Thomsen, M. Cardona, B. Friedl, I. I. Mazin, C. O. Rodriguez, and O. K. Andersen (unpublished).